FOR TECHNICAL REPORTS

NORGES TEKNISK-NATURVITENSKAPELIGE UNIVERSITET

The value of information in mineral exploration

by

Jo Eidsvik and Steinar L Ellefmo

PREPRINT
STATISTICS NO. 2/2012

NORWEGIAN UNIVERSITY OF SCIENCE AND TECHNOLOGY
TRONDHEIM, NORWAY

This report has URL http://www.math.ntnu.no/preprint/statistics/2012/S2-2012.pdf
Jo Eidsvik has homepage: http://www.math.ntnu.no/∼joeid
E-mail: joeid@stat.ntnu.no
Address: Department of Mathematical Sciences, Norwegian University of Science and Technology, N-7491 Trondheim, Norway.

The value of information in mineral exploration

Jo Eidsvik[1] **and Steinar L. Ellefmo**[2]
1) Department of Mathematical Sciences, NTNU, Norway.
2) Department of Geology and Mineral Resources Engineering, NTNU, Norway.

Corresponding author: Jo Eidsvik (joeid@math.ntnu.no), Department of Mathematical Sciences, NTNU, 7491 Trondheim, NORWAY.

Abstract

In mineral resource evaluation a careful analysis and assessments of the geology, assay data and structural data is performed. One important question is where to position the exploration boreholes, another is what method to use when analyzing the grade in the collected material. Here, a challenge of this type is whether one should analyze the collected core samples with accurate and expensive lab equipment or a simpler hand-held meter.

A dataset of about 2000 oxide observations is available, along with relevant explanatory variables, from a deposit in Norway. A Gaussian geostatistical model is used to predict the grade parameter on block support. To improve the predictions, several new boreholes are planned, giving 265 additinoal samples. The associated uncertainty reduction is evaluated, and a resource evaluation is performed with and without the planned data. Then the value of information of the planned data is computed, using assumed costs, recovery rates and revenues. The data acquired with the hand-held meter has almost the same value as the more expensive acquisition strategy; given that the already established correlation between the two datasets is proven valid.

Keywords: geostatistics, Kriging, resource classification, oxide, value of information

1 Introduction

We analyze spatial data from a deposit in Norway. The main ore mineral is a particular oxide, but the resource also contains potentially economic levels of other minerals. Several exploration boreholes have been drilled. The currently available data consist of about two thousand observations of the oxide along the boreholes. The deposit is still under consideration for mining, and the main purpose with this methodological paper is to evaluate different strategies for collecting more data.

The oxide has been measured on crushed core samples using either a X-ray fluorescence (XRF) spectrometer in the laboratory or a portable X-ray meter (XMET). The XRF data are considered to be exact measurements of the oxide, providing perfect information at the locations where they are made. The analysis procedure is time consuming. The XMET data are considered to be a noisy observation of the true oxide level, providing imperfect information. These data are acquired more time efficiently and at a lower cost than the XRF data.

We incorporate spatial dependence in the oxide by a Gaussian geostatistical model. We assume that the measurement sites (north, east and depth) are known without uncertainty, and further assume known covariates in the form of a geological rock class, representing three levels of mineralization interpreted by the geologists. As is common in geostatistics, see e.g. Cressie (1993) and Banerjee et al. (2004), we model the true oxide as a Gaussian random field (GRF) with mean values

defined by a linear regression in the covariates, and with a covariance defined by a Matern covariance function. We use maximum likelihood estimation (MLE) based on the currently available oxide data to specify the parameters of the covariance model.

The existing XRF and XMET data, and the planned data, influence the predictions and the prediction uncertainties in the spatial distribution of oxide. For a GRF the conditional covariance depends only on the data locations, the covariance model (and the covariates), and not on the actual data. As a result, it can be computed before the data are acquired. This allows us to evaluate the gain by the of planned borehole data.

In the mining industry resources are classified into measured, indicated or inferred, depending on the level of uncertainty. This is formalized through the JORC code (JORC, 2004). Since every deposit is unique, the assessment includes multiple levels of geological information, assay data, and structural data (Pilger et al., 2001). From a more methodological viewpoint, we discuss several evaluation criteria in our context, computed at a set of resource blocks. The criteria are the reduction of the marginal variances, the increase in slope and correlation, the decrease in weight of the mean (Rivoirard, 1987) and the reduction of entropy (Le and Zidek, 2006). By todays standards the final classification is done by competent persons based on these criteria, and several other case-specific criteria.

We also use the value of information (VOI) to study the potential of the data collection schemes. The VOI relates the probabilistic model to the decision about mining. The VOI is an information criterion using monetary units explicitly (Raiffa, 1968). It is defined as the difference between the prior value (before the planned data is collected) and the pre-posterior value (averaged over the planned data). The VOI is always positive because more data allows us to make better informed decisions. In practice the VOI is used to compare different data acquisition strategies over a range of prices. In our situation we can compare XRF with XMET data acquisition for different mining costs and price ranges.

The notion of VOI has been used in a number of applications recently, for instance medicine (Willan and Pinto, 2005), environment (Bouma et al., 2009) and groundwater (Trainor-Guitton et al., 2011). Similar assessements have also been done in the mining industry, see e.g. Froyland et al. (2004), Alford et al. (2007), and Phillips et al. (2009). One of our contributions in the current paper is to integrate VOI with spatial dependence in a mining context. Eidsvik et al. (2008), Bhattacharjya et al. (2010) and Martinelli et al. (2011) consider the VOI for multivariate dependent models in petroleum, but they do not use the VOI for block resource evaluation like we do here. Further, our framework gives analytical closed form solutions for the VOI in this situation.

In Section 2 we provide some background for our case study and a geostatisical model for the data. Section 3 contains the theory for spatial prediction and the various criteria for quantifying the uncertainty reduction. Section 4 presents the VOI in our case. Section 5 applies the methods to different data acquisition schemes in the oxide case study.

2 Data analysis and modeling

We first give some background on the oxide case study and perform some exploratory data analysis. Next, a geostatistical model for the data is presented.

2.1 Background and oxide data analysis

The deposit is about 2.5 km long, and is an intensively folded and lens formed body surrounded by mafic-felsic rocks. The protolith is thought to be a Proterozoic gabbroic intrusion, which has been metamorphed into the present lithologies during the Caledonian orogeny at about 400 Ma. The oxide has been formed in this process of high pressure metamorphism.

Geologists have defined three categories with increasing degree of mineralization. The classes are termed class 1, class 2 and class 3. Class 3 has the highest average oxide levels. The class 3 and class 2 categories are dominating in the central parts of the ore. The degree of mineralization is used as covariates in our analysis. The spatial classification has been done using the currently available data by site geologists.

We observe the oxide by XMET or XRF data acquired in boreholes. The laboratory XRF-data have been obtained from 10 meter long crushed sections (halves) of the core. The hand-held XMET data have been collected for every 25 cm of the core before crushing and aggregated into 10 meter long XMET-composites in correspondance with the XRF-analyses. There are 103 sites of XRF data and 1871 sites of XMET data. The 103 locations with XRF data are also measured with XMET data. Therefore, this represents a partially heterotopic sampling scheme.

Figure 1 (left) displays histograms of the oxide data collected with XMET (top) and XRF (bottom), while Figure 1 (right) shows a crossplot of the 103 (XRF, XMET) measurement pairs.

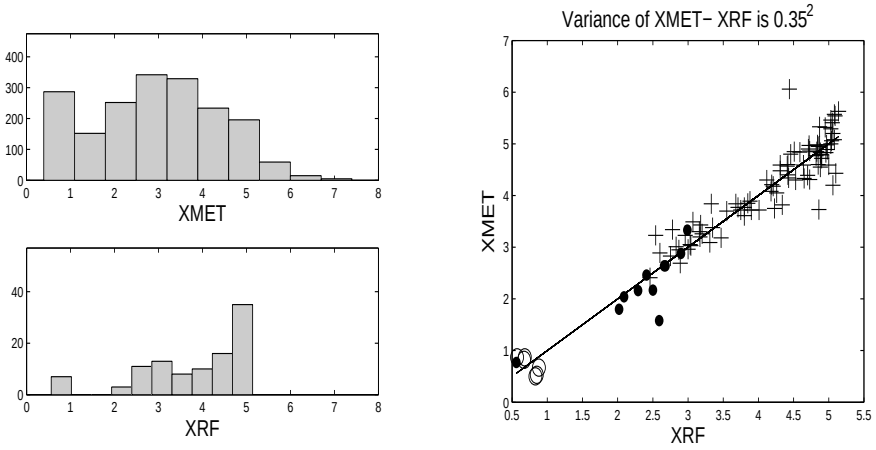

Figure 1: Left: Histogram of XMET (top) and XRF (bottom) observations. The oxide content ranges from 0.39 to 7.40 percent for XMET with a mean of 2.95. For XRF the range is from 0.56 to 5.14, with a mean of 3.80. Right: The XMET data (second axis) plotted against the XRF data (first axis) at 103 common sites.

The degree of mineralization at the measurement location is also indicated in the figure: class 1 (o), class 2 (.) and class 3 (+). The highest measurements of the oxide are typically collected at locations with class 3 covariates. For the XRF histogram in Figure 1 (left, bottom) we might notice modes representing the different classes, but there is much variability within each class.

We regress the XRF data on the class covariates $x \in \{1, 2, 3\}$ and a constant term. Using standard least squares we get a linear fit for XRF of $\hat{y} = \tilde{\beta}_0 + \tilde{\beta}_1 x$, where $\tilde{\beta}_0 = -1.10(0.39)$ and $\tilde{\beta}_1 = 1.76(0.14)$, with standard errors in parantheses. This indicates a significant relation between

the mineralization class and the oxide grade. The expected oxide responses are 0.7 (class 1), 2.4 (class 2) and 4.2 (class 3), not dissimilar to the modes visible in Figure 1.

When we treat the XRF data as perfect observations of the oxide grades, and the XMET observations as noisy measurements of the same oxide grades, it is possible to estimate the standard error of the XMET data. Using a sum of squares approach to the 103 pairs of (XRF, XMET) measurements in Figure 1 (right), we get a noise variance of XMET equal to $\hat{\tau}^2 = 0.35^2$.

2.2 Geostatistical modeling and parameter estimation

Figure 2 (left) shows the histogram of the residuals of XMET data after subtracting an ordinary least squares fit to the mineralization covariate. The residuals are close to Gaussian distributed,

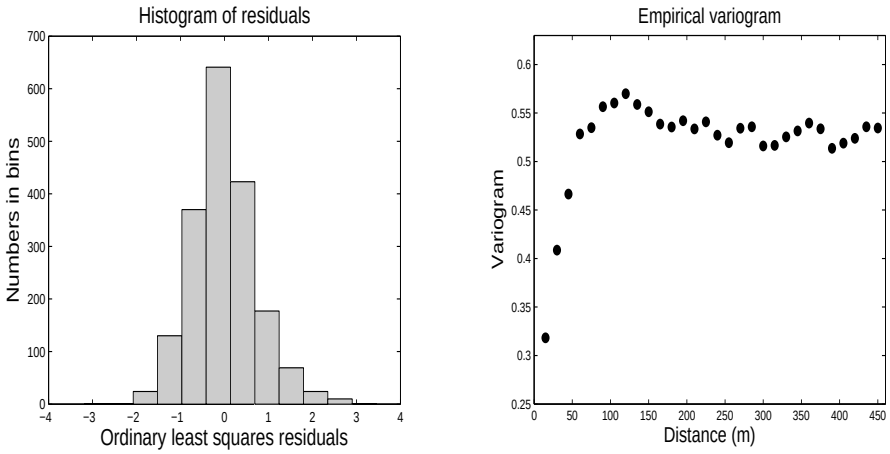

Figure 2: Left: Histogram of fitted residuals using ordinary least squares estimation for the regression parameters. Right: Empirical variogram of ordinary least squares residuals.

showing that the multimodal nature seen in Figure 1 is mainly driven by the mineralization covariate. In Figure 2 (right) we show the empirical variogram computed from the residuals. The variogram starts at about 0.25 at zero distance, and flattens out at approximately 0.55 (sill) at about 80 (range) meter distance.

We next present a joint geostatistical model for the XRF and XMET data. The XRF response ($y_1(\boldsymbol{s})$) and XMET response ($y_2(\boldsymbol{s})$) at a (north, east, depth) location $\boldsymbol{s}$ are modeled by

$$y_1(\boldsymbol{s}) = x(\boldsymbol{s}), \quad y_2(\boldsymbol{s}) = x(\boldsymbol{s}) + N(0, \tau^2).$$

Here, the true oxide at the (north, east, depth) location $\boldsymbol{s}$ is denoted $x(\boldsymbol{s})$. The XRF data provides perfect information about oxide at the location, while the XMET data is imperfect information of oxide with measurement noise variance τ^2. The noise terms are assumed to be independent from one location to another. We model the oxide as a GRF with expected value $\mu_x(s) = \boldsymbol{h}^t(\boldsymbol{s})\boldsymbol{\beta}$, where $\boldsymbol{h}^t(\boldsymbol{s})$ includes a constant term and the mineralization covariate at site $\boldsymbol{s}$, and $\boldsymbol{\beta} = (\beta_1, \beta_2)^t$ is a regression parameter. We choose a Matern covariance model to describe the spatial covariance structure of oxide. Setting the smoothness parameter of the Matern to $3/2$ we have $Cov(x(\boldsymbol{s}), x(\boldsymbol{s}')) = \sigma^2(1 + \phi h)\exp(-\phi h)$ for distance $h = ||\boldsymbol{s} - \boldsymbol{s}'||$. Then the variance

is σ^2, and ϕ indicates the strength of spatial correlation (large ϕ means faster spatial decay of the correlation). Many other covariance models could have been useful (Banerjee et al, 2004).

The collection of XRF and XMET data is denoted by $\boldsymbol{y} = (\boldsymbol{y}_1^t, \boldsymbol{y}_2^t)$, where

$$\boldsymbol{y}_1 = (y_1(\boldsymbol{s}_{1,1}), \ldots, y_1(\boldsymbol{s}_{1,103}))^t, \;\; \boldsymbol{y}_2 = (y_2(\boldsymbol{s}_{2,1}), \ldots, y_2(\boldsymbol{s}_{2,1871}))^t.$$

Here, 103 of the XMET locations equal the set of $\boldsymbol{s}_{1,1}, \ldots, \boldsymbol{s}_{1,103}$ XRF measurement locations. Using the GRF model, the 103 XRF data are represented by $\boldsymbol{y}_1 \sim N(\boldsymbol{H}_{y_1}\boldsymbol{\beta}, \boldsymbol{C}_{y_1})$, while the 1871 XMET data are represented by $\boldsymbol{y}_2 \sim N(\boldsymbol{H}_{y_2}\boldsymbol{\beta}, \boldsymbol{C}_{y_2} + \tau^2\boldsymbol{I})$. Matrices $\boldsymbol{H}_{y_1}$ and $\boldsymbol{H}_{y_2}$ consist of the explanatory variables, $\boldsymbol{h}^t(\boldsymbol{s})$, at the XRF and XMET measurement locations. The size 103×103 covariance matrix $\boldsymbol{C}_{y_1}$ describes the spatial covariance between the XRF data. The size 1871×1871 covariance matrix $\boldsymbol{C}_{y_2} + \tau^2 I$ inherits spatial correlation from the GRF and contains an additive diagonal term because of the XMET measurement noise. Altogether, we summarize the model by

$$\boldsymbol{y} \sim N(\boldsymbol{H}_y\boldsymbol{\beta}, \boldsymbol{C}_y), \quad \boldsymbol{H}_y = \begin{pmatrix} \boldsymbol{H}_{y_1} \\ \boldsymbol{H}_{y_2} \end{pmatrix}, \quad \boldsymbol{C}_y = \begin{pmatrix} \boldsymbol{C}_{y_1} & \boldsymbol{C}_{y_{1,2}} \\ \boldsymbol{C}_{y_{1,2}}^t & \boldsymbol{C}_{y_2} + \tau^2\boldsymbol{I} \end{pmatrix}, \tag{1}$$

where the size 103×1871 cross-covariance matrix between the $\boldsymbol{y}_1$ and $\boldsymbol{y}_2$ data is denoted by $\boldsymbol{C}_{y_{1,2}}$. It contains spatial covariances in the GRF model for oxide.

The currently available data $\boldsymbol{y}$ can be used to specify the unknown parameters of the model. Here, we use MLE to estimate the covariance and regression parameters. Using (1) the log-likelihood is

$$l(\boldsymbol{y}; \boldsymbol{\beta}, \sigma, \phi, \tau) = -\frac{1}{2}\log|\boldsymbol{C}_y| - \frac{1}{2}(\boldsymbol{y} - \boldsymbol{H}_y\boldsymbol{\beta})^t\boldsymbol{C}_y^{-1}(\boldsymbol{y} - \boldsymbol{H}_y\boldsymbol{\beta}). \tag{2}$$

For fixed covariance parameters the MLE of $\boldsymbol{\beta}$ is analytically available:

$$\hat{\boldsymbol{\beta}}_y = \boldsymbol{S}_y\boldsymbol{H}_y^t\boldsymbol{C}_y^{-1}\boldsymbol{y}, \quad \boldsymbol{S}_y = (\boldsymbol{H}_y^t\boldsymbol{C}_y^{-1}\boldsymbol{H}_y)^{-1}. \tag{3}$$

In order to compute the MLE of the covariance parameters we use a Fisher-scoring updating scheme, where the $\hat{\boldsymbol{\beta}}_y$ estimate is also updated at every iteration of the procedure, see e.g. Mardia and Marshall (1984). After some Fisher-scoring iterations, the parameter values converge to the MLE $\hat{\sigma}$, $\hat{\phi}$ and $\hat{\tau}$. Suitable starting values for the covariance parameters are obtained from the empirical variogram in Figure 2 (right).

The covariance of the estimator $\hat{\boldsymbol{\beta}}_y$ is given by $\boldsymbol{S}_y$ in (3), evaluated as a function of the MLEs $\hat{\sigma}$, $\hat{\phi}$ and $\hat{\tau}$, which are plugged into the covariance matrix $\boldsymbol{C}_y$. The asymptotic covariance of $(\hat{\sigma}, \hat{\phi}, \hat{\tau})$ is the inverse second derivative of the log-likelihood l in (2) with respect to σ, ϕ and τ. For our dataset the MLEs are $\hat{\beta}_0 = -0.18$ (0.07) and $\hat{\beta}_1 = 1.32$ (0.03), and $\hat{\sigma} = 0.62$ (0.02), $\hat{\phi} = 0.095$ (0.006), and $\hat{\tau} = 0.45$ (0.02). The standard errors are in parantheses. Note that the regression parameter estimates based on both XRF and XMET data, and using the spatial model, differs from the standard least squares estimates based on XRF data alone.

3 Uncertainty reduction obtained by drilling more boreholes

A mineral resource is a concentration or occurrence of material of intrinsic economic interest in or on the Earth's crust in such form, quality and quantity that there are reasonable prospects

for eventual economic extraction (JORC, 2004). Dependent on the level of confidence in the geological data, the data density and data configuration, a mineral resource can be categorized as inferred, indicated and measured (with decreasing uncertainty). An ore reserve is the economically mineable part of a measured and/or indicated mineral resource. When doing the transition from a resource to a reserve, a number of modifying factors are applied. Examples of such factors are mining- and beneficiation methods, legal- and environmental issues, market-, social- and governmental factors. The deposit in question can potentially be mined in an open pit, possibly going underground at a later stage. The decisions about opening the mine and choosing mining strategies depend on all modifying factors. We focus on quantitative approaches based on the geostatistical modeling.

A resource will be classified into the different categories by a competent person. She or he is a member of a recognized professional organization and has sufficient relevant experience. The classification will be done based on a detailed understanding of the mineralization and on uncertainty indicators. What indicators to use are deposit specific and in practice the choice of the competent person, and we will not try to draw any conclusions here.

We define 3740 resource blocks of size 20^3 m^3 inside a possible pit where we predict the oxide grade. The oxide grade in a block is denoted $\boldsymbol{x} = (x(\boldsymbol{s}_{0,1}), \ldots, x(\boldsymbol{s}_{0,n_b}))^t$, where $n_b = 64$ is the block discretization in our case. The final grade estimate in a block is the average of the n_b in-block estimates.

Recall that the currently available data $\boldsymbol{y}$ consists of 1871 XMET and 103 XRF observations. The mining company considers acquiring more XRF or XMET data. About 20 new boreholes have been planned, giving 265 additional measurements of either XRF or XMET data. We denote this new data by $\boldsymbol{z} = (z(\boldsymbol{s}_{z,1}), \ldots, z(\boldsymbol{s}_{z,265}))^t$.

The design of boreholes should cover the resource adequately. If a block is very close to a borehole, we expect low uncertainty in this block. When we move away from a borehole, the uncertainty increase. Without the planned data $\boldsymbol{z}$, these distances are obviously larger. In addition to distances, it is preferable to have data in different directions (azimuths), since these data will carry more information about small scale trends and the prediction reflects interpolation rather than extrapolation. When we collect the new data $\boldsymbol{z}$, we cover more directions. Note that the locations of the planned data are already determined. As part of the evaluation, we will remove individual boreholes from the analysis, but we will not consider the spatial design problem here (Zimmerman, 2006).

3.1 Spatial prediction and prediction variance

Distance or angle criteria do not include geostatistical knowledge, such as the uncertainty level or degree of spatial correlation. A natural starting point for optimal geostatistical prediction is the joint distribution of $\boldsymbol{x}$, $\boldsymbol{z}$, and $\boldsymbol{y}$. Given the parameter $\boldsymbol{\beta}$ and the covariance model, this distribution is the multivariate Gaussian:

$$\begin{pmatrix} \boldsymbol{x} \\ \boldsymbol{z} \\ \boldsymbol{y} \end{pmatrix} \sim N\left[\begin{pmatrix} \boldsymbol{H}_x \\ \boldsymbol{H}_y \\ \boldsymbol{H}_z \end{pmatrix} \boldsymbol{\beta}, \begin{pmatrix} \boldsymbol{C}_x & \boldsymbol{C}_{x,y} & \boldsymbol{C}_{x,z} \\ \boldsymbol{C}_{x,y}^t & \boldsymbol{C}_y & \boldsymbol{C}_{y,z} \\ \boldsymbol{C}_{x,z}^t & \boldsymbol{C}_{y,z}^t & \boldsymbol{C}_z \end{pmatrix} \right], \tag{4}$$

where $\boldsymbol{C}_x$ denotes the covariance matrix for the block grade variables, while $\boldsymbol{C}_z$ is the covariance matrix of the new data $\boldsymbol{z}$. If $\boldsymbol{z}$ represents XMET data, the latter covariance matrix has a spatial part

and an additive diagonal part with the nugget effect τ^2. If $\boldsymbol{z}$ represents XRF data, this is perfect information, and there is no nugget effect in $\boldsymbol{C}_z$. The cross-covariance matrices $\boldsymbol{C}_{x,z}$, $\boldsymbol{C}_{x,y}$ and $\boldsymbol{C}_{y,z}$ are calculated using the spatial covariance model for the oxide grade.

The conditional mean of $\boldsymbol{x}$ and $\boldsymbol{z}$ given current data $\boldsymbol{y}$ is

$$\boldsymbol{\mu}_{x|y} = \boldsymbol{H}_x\hat{\boldsymbol{\beta}}_y + \boldsymbol{C}_{x,y}\boldsymbol{C}_y^{-1}(\boldsymbol{y} - \boldsymbol{H}_y\hat{\boldsymbol{\beta}}_y), \quad \boldsymbol{\mu}_{z|y} = \boldsymbol{H}_z\hat{\boldsymbol{\beta}}_y + \boldsymbol{C}_{y,z}^t\boldsymbol{C}_y^{-1}(\boldsymbol{y} - \boldsymbol{H}_y\hat{\boldsymbol{\beta}}_y),$$

where we simply plug in the regression parameter estimate $\hat{\boldsymbol{\beta}}_y$. We also plug in covariance parameters $\hat{\sigma}$, $\hat{\phi}$ and $\hat{\tau}$ in all covariance and cross-covariance matrices. When we write out the regression parameter $\hat{\boldsymbol{\beta}}_y$ as a function of the data $\boldsymbol{y}$, we get

$$\boldsymbol{\mu}_{x|y} = \left(\boldsymbol{M}_{x,y}\boldsymbol{S}_y\boldsymbol{H}_y^t + \boldsymbol{C}_{x,y}\right)\boldsymbol{C}_y^{-1}\boldsymbol{y}, \quad \boldsymbol{\mu}_{z|y} = \left(\boldsymbol{M}_{z,y}\boldsymbol{S}_y\boldsymbol{H}_y^t + \boldsymbol{C}_{y,z}^t\right)\boldsymbol{C}_y^{-1}\boldsymbol{y}, \tag{5}$$

where $\boldsymbol{M}_{x,y} = \boldsymbol{H}_x - \boldsymbol{C}_{x,y}\boldsymbol{C}_y^{-1}\boldsymbol{H}_y$ and $\boldsymbol{M}_{z,y} = \boldsymbol{H}_z - \boldsymbol{C}_{y,z}^t\boldsymbol{C}_y^{-1}\boldsymbol{H}_y$.

Under the Gaussian modeling assumptions, the kriging predictor in (5) is optimal, i.e. the unbiased predictor with minimum variance. In practice predictions based on a search ellipsoid are commonly used. One reason for constructing search ellipsoids is computational efficiency, but in our case the data size is not that massive. Another reason could be non-stationarity, but then there are no clear approaches for consistently making search ellipsoids and assessing parameter estimates of a non-stationary geostatistical model. We have chosen to use all data in our evaluations here.

While it is hard to include the uncertainty of the covariance parameters in (5), we can easily account for the uncertainty in the regression parameters $\hat{\boldsymbol{\beta}}_y$, see e.g. Cressie (1993). The resulting conditional covariance expressions are

$$\boldsymbol{C}_{x|y} = \boldsymbol{C}_x - \boldsymbol{C}_{x,y}\boldsymbol{C}_y^{-1}\boldsymbol{C}_{x,y}^t + \boldsymbol{M}_{x,y}\boldsymbol{S}_y\boldsymbol{M}_{x,y}^t, \quad \boldsymbol{C}_{z|y} = \boldsymbol{C}_z - \boldsymbol{C}_{y,z}^t\boldsymbol{C}_y^{-1}\boldsymbol{C}_{y,z} + \boldsymbol{M}_{z,y}\boldsymbol{S}_y\boldsymbol{M}_{z,y}^t, \tag{6}$$

where the last terms with $\boldsymbol{M}_{x,y}$, $\boldsymbol{M}_{z,y}$ and $\boldsymbol{S}_y$ compensate for the increased variability caused by estimating $\boldsymbol{\beta}$.

Denote the average block grade by $\bar{x} = \sum_i x_i/n_b$. We denote the Gaussian density of $\bar{x}$ given $\boldsymbol{y}$ by $\pi(\bar{x}|\boldsymbol{y}) = N(\mu_{\bar{x}|y}, C_{\bar{x}|y})$. This is computed for every resource block, and we define Std_y as the length 3740 vector of Kriging standard errors ($\sqrt{C_{\bar{x}|y}}$), conditional on the current data $\boldsymbol{y}$.

The procedures can be extended to include both current data $\boldsymbol{y}$ and $\boldsymbol{z}$. The conditional mean of $\boldsymbol{x}$, given both data, is

$$\boldsymbol{\mu}_{x|yz} = \boldsymbol{\mu}_{x|y} + \boldsymbol{C}_{x,z|y}\boldsymbol{C}_{z|y}^{-1}(\boldsymbol{z} - \boldsymbol{\mu}_{z|y}), \tag{7}$$

where $\boldsymbol{C}_{x,z|y}$ is the covariance of $\boldsymbol{x}$ and $\boldsymbol{z}$, given $\boldsymbol{y}$. This conditional mean is a linear function of the prospective data $\boldsymbol{z}$. Note that the regression parameter estimator $\hat{\boldsymbol{\beta}}_{yz}$ computed from all data and all covariates $\boldsymbol{H}_{yz}^t = [\boldsymbol{H}_y^t\boldsymbol{H}_z^t]$ is linear in $\boldsymbol{z}$. The associated covariance is $\boldsymbol{S}_{yz} = [\boldsymbol{H}_{yz}^t\boldsymbol{C}_{yz}^{-1}\boldsymbol{H}_{yz}]^{-1}$, and this can be accounted for in the prediction variance given all data. Just like in the situation with only current data $\boldsymbol{y}$, we define Std_{yz} as the Kriging standard errors of average block grades, now given both $\boldsymbol{y}$ and $\boldsymbol{z}$ data. The reduction in prediction variance depends on the locations of the new observations $\boldsymbol{z}$, relative to each other, and to the current data $\boldsymbol{y}$ and the resource blocks $\boldsymbol{x}$. Collecting XRF data in the planned boreholes provides a larger reduction in prediction variance than with XMET, but in general the uncertainty reduction is a complicated function of the covariance parameters.

3.2 Slope, correlation and weight of the mean

Rivoirard (1987) uses the regression between the predicted and true block grades, called the slope, to assess the effects of different Kriging neighborhoods. This criterion has also been used to quantify the degree of measured or indicated resources in mining (Vann et al., 2003). For each resource block we have

$$\text{Slope}_y = \text{Cov}(\bar{x}, \mu_{\bar{x}|y})/\text{Var}(\mu_{\bar{x}|y}) = (\boldsymbol{w}^t \boldsymbol{G}_{x,y} \boldsymbol{C}_y^{-1} \boldsymbol{C}_{x,y}^t \boldsymbol{w})/(\boldsymbol{w}^t \boldsymbol{G}_{x,y} \boldsymbol{C}_y^{-1} \boldsymbol{G}_{x,y}^t \boldsymbol{w}), \tag{8}$$

where $\boldsymbol{w}^t = \mathbf{1}^t/n_b$ and $\mathbf{1}$ is a vector of ones. Moreover, $\boldsymbol{G}_{x,y} = \boldsymbol{M}_{x,y}\boldsymbol{S}_y\boldsymbol{H}_y^t + \boldsymbol{C}_{x,y}$ is recognized in (5). The correlation is a normalized version of the slope;

$$\text{Corr}_y = \text{Corr}(\bar{x}, \mu_{\bar{x}|y}) = \text{Slope}_y \cdot \sqrt{\text{Var}(\mu_{\bar{x}|y})/\text{Var}(\bar{x})}. \tag{9}$$

The weight of the mean (Rivoirard, 1987) is another useful quality indicator in kriging, see Vann et al. (2003). Given data $\boldsymbol{y}$, the weight of the mean is interpreted as the relative impact of the regression, compared with that of the simple Kriging predictor $\boldsymbol{C}_{x,y}\boldsymbol{C}_y^{-1}\boldsymbol{y}$. From the prediction formula in (5) we recognize the simple Kriging predictor as the last term, and the regression effect in the first part. When the deposit is more densely sampled, the second term will dominate over the first term. We have

$$\text{Weight}_y = (\boldsymbol{w}^t \boldsymbol{M}_{x,y}\boldsymbol{S}_y\boldsymbol{H}_y^t\boldsymbol{C}_y^{-1}\mathbf{1})/[(\boldsymbol{w}^t \boldsymbol{M}_{x,y}\boldsymbol{S}_y\boldsymbol{H}_y^t\boldsymbol{C}_y^{-1}\mathbf{1}) + (\boldsymbol{w}^t \boldsymbol{C}_{x,y}\boldsymbol{C}_y^{-1}\mathbf{1})]. \tag{10}$$

The slope, correlation and weight of the mean are computed for each resource block. In total, they can be represented as length 3740 vectors, with one value for each resource block. They can be defined similarly conditioning on both current data $\boldsymbol{y}$ and the new data $\boldsymbol{z}$. When we get more accurate predictions of the grade, the slope is closer to 1, the correlation is closer to 1, while the weight of the mean is closer to 0. The effect is expected to be clearer with perfect information (XRF) than with imperfect data (XMET).

4 Information criteria

We next discuss criteria treating all blocks jointly, and let $\boldsymbol{x}^*$ denote the oxide variable at the center of each of the 3740 resource blocks. We compare the information content using the entropy or the prior or pre-posterior value (and VOI) of current data $\boldsymbol{y}$ and prospective data $\boldsymbol{z}$.

4.1 Reduction of entropy

Entropy is a very common measure of information content, see e.g. Cover and Thomas (1991), Le and Zidek (2006) and Wellmann et al. (2011) for a spatial perspective. The entropy (disorder) decreases with more information. It is defined as the negative expected value of the log density. For a Gaussian $\pi(\boldsymbol{x}^*) = N(\boldsymbol{\mu}, \boldsymbol{\Sigma})$ we have entropy

$$\text{Ent}(\boldsymbol{x}^*) = -\int \pi(\boldsymbol{x}^*)\log\pi(\boldsymbol{x}^*)d\boldsymbol{x} = \frac{n}{2}\log(1+2\pi) + \frac{1}{2}\log|\boldsymbol{\Sigma}|. \tag{11}$$

The entropy reduction when acquiring the new data $\boldsymbol{z}$ becomes $\delta\text{Ent} = \text{Ent}(\boldsymbol{x}^*|\boldsymbol{y}) - \text{Ent}(\boldsymbol{x}^*|\boldsymbol{y},\boldsymbol{z}) = \frac{1}{2}(\log|\boldsymbol{C}_{x^*|y}| - \log|\boldsymbol{C}_{x^*|yz}|)$, where $\boldsymbol{C}_{x^*|y}$ is the covariance at all resource blocks given $\boldsymbol{y}$, while

$\boldsymbol{C}_{x^*|yz}$ is conditional on both $\boldsymbol{y}$ and $\boldsymbol{z}$ data. The determinant expressions can be evaluated before the actual data are collected.

Note that the entropy is a scalar. The reduction in entropy can thus be regarded as a univariate summary of the information associated with the (updated) distribution. Just like for the other criteria introduced in Section 3, it is hard to relate the entropy to costs and revenuess, see e.g. Chapter 11 in Le and Zidek (2006).

4.2 Value of information of drilling more boreholes

The VOI is the maximum monetary amount a decision maker should pay to collect data. By tying money and the actual decision makin to the statistical model, the VOI goes beyond mere uncertainty reduction. In our context there are two levels of decisions. The downstream decision is whether to open the mine or not. This question is incorporated to solve for the second level of decisions; whether one should collect XMET or XRF data in the planned boreholes, or no further data. If the VOI is larger than the price of the XMET or XRF data, we decide to purchase more data.

Within a decision analytic framework, the VOI is computed before data acquisition, using the expected revenues and costs from the mine. It is defined as the difference between prior and pre-posterior value. The VOI is always positive, since the pre-posterior value computation gives us the chance to make better informed decisions, on average. When we compute the VOI, we make certain assumptions about the mining strategy. First, we assume that one either mines the entire set of resource blocks for oxide, or nothing at all. This would neglect the value of being able to change the strategy along the way. This is inherent in the real option approach, see e.g. Martinez (2009), but not taken into account here. Next, we assume there is a fixed cost for mining one ton of oxide ore, and this is the same for all blocks. In addition, the blocks with a estimated grade above cut-off are processed after mining, whereas the waste rock (estimated grade below cut-off) is not processed any further. This means that a fixed fraction of the blocks contain possible revenues, but that there are costs associated with all blocks.

Let r_l be the revenue factor associated with resource block $l = 1, \ldots, 3740$, which gives the estimated revenue once it is multiplied with the estimated grade. We set r_l to 0 outside the ore, since these blocks are not processed further. The revenue level r_l is the product of the price of product extracted from the oxide, block volume and certain processing parameters. Let further k_l be the cost of mining and processing a resource block. If block l is waste rock, the cost of processing is not included in k_l. We discuss both r_l and k_l further in the examples below. Let $\boldsymbol{r} = (r_1, \ldots, r_{3740})^t$ be the vector of revenue levels, and $\boldsymbol{k} = (k_1, \ldots, k_{3740})^t$ the costs in the set of resource blocks. The prior value is computed based on the currently available data $\boldsymbol{y}$:

$$\text{PV} = \max(p_y, 0), \;\; p_y = \boldsymbol{r}^t \boldsymbol{\mu}_{\boldsymbol{x}^*|y} - \boldsymbol{k}^t \boldsymbol{1}, \tag{12}$$

where $\boldsymbol{\mu}_{\boldsymbol{x}^*|y}$ is the prediction of the oxide grades given the current data $\boldsymbol{y}$. Here, the risk neutral mining company decides to develop the mine when the expected profit p_y is positive.

Consider now what happens when we collect more data $\boldsymbol{z}$. The new data $\boldsymbol{z}$ are either XMET or XRF in the planned boreholes. The pre-posterior value is

$$\text{PoV} = \int_{\boldsymbol{z}} \max(p_{yz}, 0) \pi(\boldsymbol{z}|\boldsymbol{y}) d\boldsymbol{z}, \;\; p_{yz} = \boldsymbol{r}^t \boldsymbol{\mu}_{\boldsymbol{x}^*|yz} - \boldsymbol{k}^t \boldsymbol{1}, \tag{13}$$

where $\boldsymbol{\mu}_{\boldsymbol{x}^*|yz}$ is the prediction of the grades given the current data $\boldsymbol{y}$ and planned data $\boldsymbol{z}$. We integrate over all possible prospective data outcomes $\boldsymbol{z}$. The density of the planned data $\boldsymbol{z}$, denoted $\pi(\boldsymbol{z}|\boldsymbol{y}) = N(\boldsymbol{\mu}_{z|y}, C_{z|y})$, is defined by (5) and (6). The VOI is

$$\text{VOI} = \text{PoV} - \text{PV}.$$

We decide to purchase the data $\boldsymbol{z}$ if the VOI is larger than the price of data acquisition. The XRF data is perfect information, and the VOI of XRF is always larger than the VOI of the imperfect XMET data. However, the XRF data has a higher price than the imperfect XMET data.

The VOI is also commonly used to compare different acquisition schemes. Say we had a budget forcing us to drill less boreholes. Then VOI can help us decide where to focus, i.e. which boreholes to drill. Similarly, one could compare the VOI of XMET data at all boreholes with the VOI of XRF over a subset of boreholes.

With the Gaussian modeling assumptions, the pre-posterior value is analytically available. This was shown for the univariate situation in Bickel (2008). Here, to get the PoV, we must solve an integral over the multivariate prospective data $\boldsymbol{z}$ in (13). However, the only relevant function of $\boldsymbol{z}$ is the linear combination defined as the decision variable $p = p_{yz} = \boldsymbol{r}^t\boldsymbol{\mu}_{\boldsymbol{x}^*|yz} - \boldsymbol{k}^t\mathbf{1}$, which enters in (13). The remaining 264 dimensions of the $\boldsymbol{z}$ variable are irrelevant for the decision. Given the current data $\boldsymbol{y}$, the decision variable p, being a linear function of $\boldsymbol{z}$ as in (7), has a univariate Gaussian distribution

$$\pi(p|\boldsymbol{y}) = N(\mu_p, \sigma_p^2), \;\; \mu_p = \boldsymbol{r}^t\boldsymbol{\mu}_{\boldsymbol{x}^*|y} - \boldsymbol{k}^t\mathbf{1}, \;\; \sigma_p^2 = \boldsymbol{r}^t\boldsymbol{C}_{\boldsymbol{x}^*,z|y}\boldsymbol{C}_{z|y}^{-1}\boldsymbol{C}_{\boldsymbol{x}^*,z|y}^t\boldsymbol{r},$$

where the mean and covariances are defined from the joint Gaussian of $(\boldsymbol{x}^{*t}, \boldsymbol{y}^t, \boldsymbol{z}^t)^t$ similar to that in (4). For the covariances expressions in σ_p^2, we additionally account for uncertainty in the regression parameter estimator $\hat{\boldsymbol{\beta}}_{yz}$, similar to what was done in Section 3.

The pre-posterior value becomes

$$\begin{aligned}
\text{PoV} &= \int_{R^n} \max\left(\boldsymbol{r}^t\boldsymbol{\mu}_{\boldsymbol{x}^*|yz} - \boldsymbol{k}^t\mathbf{1}, 0\right)\pi(\boldsymbol{z}|\boldsymbol{y})d\boldsymbol{z} = \int_{-\infty}^{\infty}\max(p,0)\pi(p|\boldsymbol{y})dp \\
&= \int_{p>0} p\frac{1}{\sqrt{2\pi\sigma_p^2}}\exp\left(-\frac{(p-\mu_p)^2}{2\sigma_p^2}\right)dp = \int_{v>-\mu_p/\sigma_p}(\mu_p + v\sigma_p)\frac{1}{\sqrt{2\pi}}\exp\left(-\frac{v^2}{2}\right)dv \\
&= \mu_p[1-\Phi(-\mu_p/\sigma_p)] - \sigma_p\left[\frac{1}{\sqrt{2\pi}}\exp\left(-\frac{v^2}{2}\right)\right]_{-\mu_p/\sigma_p}^{\infty} \\
&= \mu_p[1-\Phi(-\mu_p/\sigma_p)] + \sigma_p\phi(-\mu_p/\sigma_p) \\
&= \mu_p\Phi(\mu_p/\sigma_p) + \sigma_p\phi(\mu_p/\sigma_p), \qquad (14)
\end{aligned}$$

where $\phi(\cdot)$ is the probability density function and $\Phi(\cdot)$ the cumulative distribution function of the standard Gaussian. The derivation in (14) uses a transformation of variables, $p = \mu_p + v\sigma_p$, and symmetry properties of the standard Gaussian distribution for v. Moreover, we use that $\int v\exp(-\frac{v^2}{2})dv = -\exp(-\frac{v^2}{2}) + \text{constant}$. Using this analytical result and (12), the resulting VOI in (14) becomes $\text{VOI} = \mu_p\Phi(\mu_p/\sigma_p) + \sigma_p\phi(\mu_p/\sigma_p) - \max(p_y, 0)$.

5 Results and discussion

We now evaluate the planned boreholes using the different criteria for uncertainty reduction (Section 5.1), resource classification (Section 5.2) and VOI (Section 5.3). In Section 5.4 we study

the influence of individual boreholes.

5.1 Uncertainty reduction by XRF or XMET information

Figure 3 shows predictions (b) and prediction uncertainty (c) of the oxide grade along a depth profile along a north-east line (a). The predictions and prediction uncertainties are conditional on the current data $\boldsymbol{y}$. In Figure 3 a) we show the current XRF data locations (crossed), the current

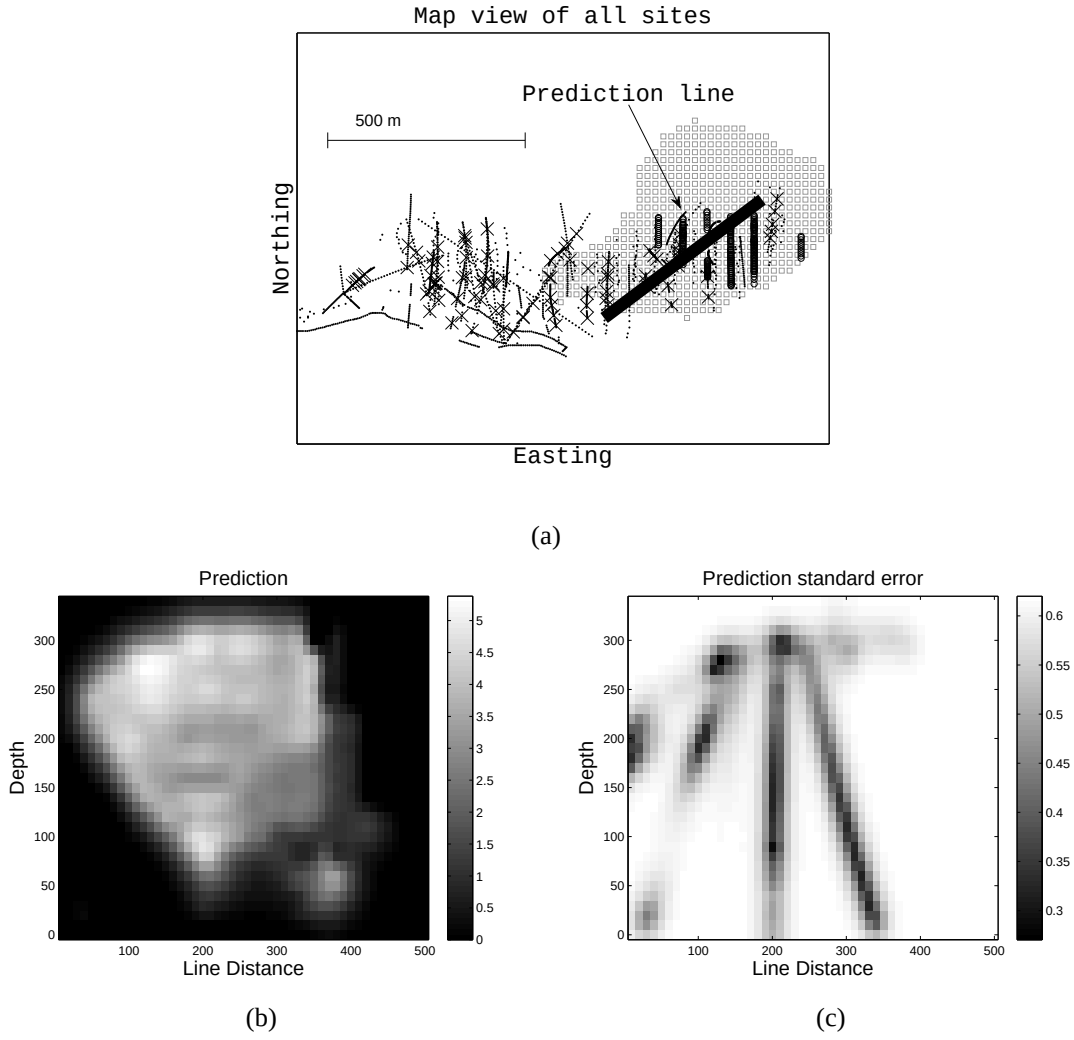

Figure 3: Predictions of the oxide grade in % in (b) and prediction uncertainties in (c) along the vertical profile illustrated by the NE-SW-trending line shown in (a). Both predictions and the standard errors are based on the currently available borehole data.

XMET data locations (dots), the planned borehole locations (circles), and the locations of the resource blocks (square). The prediction in Figure 3 b) shows high levels of oxide in the ore zone. The prediction variance is naturally smallest in the vicinity of current boreholes. Note that the planned data are in the selected pit region. With the additional measurements, the prediction

uncertainty along the selected line, and in the blocks as a whole, would go down. We will next quantify this uncertainty reduction.

Table 1 shows the values of different evaluation criteria. The XRF data are of course more in-

Table 1: Various evalaution criteria: Distance to nearest borehole, Kriging std, slope, correlation, weight of mean and entropy, using current data, and with planned XRF and XMET borehole data. The distance, standard error, slope and weight of the mean are vectors for all resource blocks. Here, we display the averages over all blocks.

	distance	std	slope	corr	weight of mean	entropy
Current data	55.1	0.59	0.62	0.21	0.73	Ent=-2930
XMET data	48.0	0.57	0.69	0.27	0.63	δEnt=43.0
XRF data	48.0	0.57	0.70	0.29	0.62	δEnt=72.4

formative than XMET data, and for some criteria we clearly gain some by acquiring XRF instead of XMET data. For instance, the reduction in entropy is almost twice as large when collecting XRF. Of course, a pure distance criterion does not separate between XRF and XMET in the new boreholes. For the Kriging std the average difference between XRF and XMET collection is miniscule. There is a slight improvement in the slope, correlation and weight of the mean criteria, but the added value of XRF, compared with XMET, is small considering the reduction from the current data.

Figure 4 illustrates the variability in the Kriging standard error, slope, correlation and the weight of mean at the 3740 resource blocks. The histograms show current values (left), with XMET data (middle) and with XRF data (right). Clearly, more data pushes the histogram of the standard errors (top) towards smaller values, the slope and correlation (middle) to higher values, and the weight of the mean (bottom) to smaller values. Thus, at many resource blocks there is clearly added information in the planned borehole data. The improvement going from XMET to XRF is visible for resource blocks close to the planned boreholes, but not far away from these locations. In fact, the Kriging prediction errors have larger variability after conditioning on more information. Of course, the planned data acquisition is guided to the spatial domains of most interest, and the reduction of uncertainty is highest where we want to predict the grade accurately.

5.2 Resource classification

A resource classification is based on multiple criteria and experience of the local geology, usually evaluated by a so-called competent person. Here, we simply compare the presented geostatistical criteria and classify based on thresholding. It is not an attempt to do a resource classification in compliance with the JORC-code. The categorization limits are obtained from the currently available data using geometric considerations as follows: For each resource block we compute the azimuth angles and distances to the five nearest borehole measurement locations. These are used to group the resource blocks in four categories: Category 1: The fifth closest point is within 30m and the standard deviation of the azimuth angles to data locations within 100 m is between 80 and 130 degrees. Category 2: The fifth closest point is between 30m and 60m and the standard deviation of the azimuth angles to data locations within 100 m is between 80 and 130 degrees. Category 3: The fifth closest point is within 60m and 200m and the standard deviation of the azimuth angles to data locations within 100 m is between 80 and 130 degrees. Category 4 is defined by the remaining

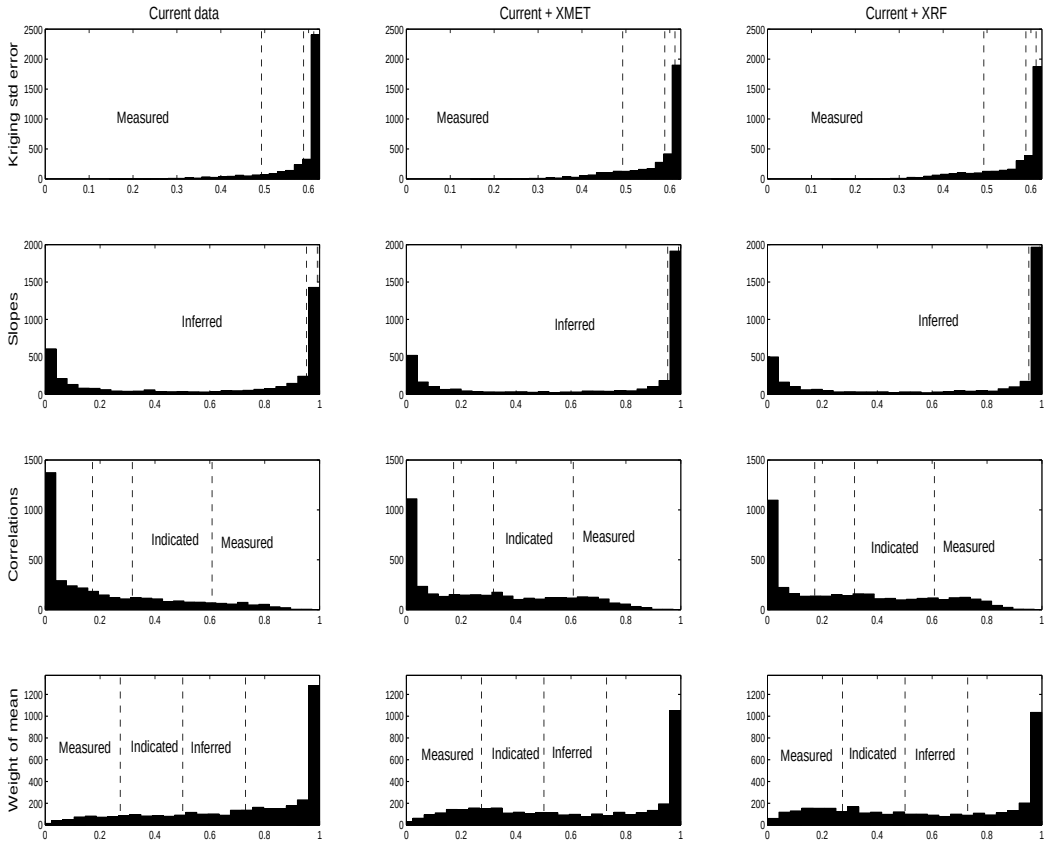

Figure 4: Histogram of evaluation criteria at all resource blocks. Kriging standard errors (top), slope (middle, top), correlation (middle, bottom) and weight of the mean (bottom). The left displays are based on current data, middle displays on current data and XMET in planned boreholes and right displays on current data and XRF in planned boreholes. The vertical dashed lines are the criteria-based separation of measured, indicated and inferred resources.

resource blocks. The azimuth variability condition ensures that there are proximal measurements in more directions, not only one borehole. Given this categorization of resource blocks, the 75 percentiles of all criteria are computed from the Kriging errors, slopes, correlation and weight of the mean in resource blocks belonging to each category. These values define the thresholding values for measured, indicated and inferred. They are displayed by vertical dashed lines in Figure 4. Recall that this is based on the current boreholes. The same thresholds are next applied for the planned data as well.

The categorization we have done here is used to study the information content in the new data and allows us to compare the methodologies. In particular, we aim to study the effects of XMET and XRF data acquisition in the planned boreholes. The geometric criteria based on distances and angles is easy to understand, but it is not useful to compare the XRF and XMET data, since they are equally informative in terms of distances and angles.

In Table 2 we show the resulting tonnages in the measured, indicated and inferred categories. Here, the resource blocks falling in the measured, indicated and inferred categories are converted to

Table 2: Resource classification (in million tonnes) based on current data, XMET data in planned boreholes and XRF data in planned boreholes. The measured, indicated and inferred classification is done from thresholds in different evaluation criteria: Distances, kriging standard deviations, slope, correlation and weight of mean.

	Distance	Kriging Std	Slope	Corr	Weight
	Current data				
Measured	9.0	8.8	8.8	8.8	8.5
Indicated	20.8	21.3	21.9	21.2	21.4
Inferred	10.6	10.4	9.8	10.5	10.6
	Current data and XMET in planned boreholes				
Measured	13.8	14.2	15.1	14.2	15.2
Indicated	21.6	21.5	21.0	21.4	20.0
Inferred	5.1	4.8	4.5	5.0	5.4
	Current data and XRF in planned boreholes				
Measured	13.8	15.0	16.0	15.0	16.7
Indicated	21.6	21.0	20.4	20.8	18.7
Inferred	5.1	4.6	4.2	4.8	5.1

tonnes of resource. The block volumes outside the ore are not included in the calculation. We use a cut-off value of 2.5 % (based on current data) to separate waste from ore. With the current data, using the Kriging standard error as criterion, there are about 9 million tonnes of measured resource and 20 million tonnes indicated. There are only slight variations between the criteria using our thresholding method. Obviously, with more data, there are more resource blocks in the measured category. When we collect XMET data in the planned boreholes, the measured category in Table 2 has around 14-15 million tonnes. The indicated category is around 21 million tonnes. Some blocks have gone from indicated to measured, while others have gone from inferred to indicated. The sum of measured and indicated resources is close to 40 million tonnes. Collecting XRF data in the planned boreholes gives only slightly larger numbers in the measured category: 15-17 million tonnes. Note that the pure geometric distance criterion has the same number as for XMET (13.8 million tonnes measured), since it uses no uncertainty modeling. The indicated resource blocks are about 19-21 million tonnes. In summary, there is a clear increase in measured tonnages going from current to XMET, but not such an improvement when collecting XRF data instead of XMET.

Recall that these numbers are based on our subjective criteria. A real-life resource classification would have been based performed by a competent person in compliance with the JORC-code or other similar codes.

5.3 Value of XMET or XRF information

In order to assess the value of XMET and XRF information, we need to specify revenues, costs, processing parameters and tonnages. In the following we present our assumed levels for costs, revenues and recovery rates. These would be subject to change based on the market level. The performance in the mining and processing processes are mainly dependent on three factors.

These factors are the mining recovery (here set to 95 %), the recovery from the beneficiation, i.e. separating mineral from gangue in the processing oplant (here set to 55 %), and the dilution in the pit (here set to 5 %). The density (3.38 ton/m^3) of the ore is assumed known and independent of the grade. The block volume is $V = 20$ m^3 for a full block inside the ore. We play with the market price for the oxide, setting a low level of \$ 720 per ton, intermediate level of \$ 770 per ton, and high \$ 820 per ton. These inputs define a revenue factor which gives the estimated income from a block when it is multiplied with the predicted grade. The block revenue factor for the oxide is then $r_l = 770 \cdot 0.95 \cdot 0.55 \cdot (1 - 0.05) \cdot 3.38 \cdot 20 = \$\ 10.3$ million, assuming the intermediate price level and no void volume outside the final pit. Assuming a block with a oxide-grade of 4 %, the estimated revenue from the block is $0.04 \cdot 10.3 = \$\ 0.41$ million.

The operating costs in the mine (pit) for an ore block are set to \$ 3 per ton, whereas the processing costs in th beneficiation plant are assumed to be \$ 8 per ton. A block of ore will thus cost $k_l = 11 \cdot 3.38 \cdot V = \$\ 0.30$ million in mining and processing, giving a profit of $0.41 - 0.30 = \$\ 0.11$ million per block when the grade of oxide is 4 %. A block of waste will be drilled, blasted, loaded and transported, but instead of being transported to the processing plant, it will be deposited. The operating cost for this treatment is assumed to be \$ 3 per ton, i.e the cost per block of waste rock is $k_l = 3 \cdot 3 \cdot V = \$\ 0.07$ million, where the density of waste rock is set to 3 ton/m^3. Out of the 3740 blocks, there are 1676 ore blocks, while the rest is waste rock. Again, 2.5 % is used as a cut-off alue, separating waste from ore.

Below we will study sensitivity to different cost and processing parameters. Using the above inputs, the intrinsic value of the oxide is estimated to - \$ 38 million when the oxide product price is low, -\$ 2 million when the oxide product price is intermediate, and \$ 35 million when the oxide product price is high. In the first two situations the associated a priori values become 0. The posterior value is always higher than this, but only significantly larger in the intermediate situation. Then, the VOI of XMET data in the planned boreholes is \$ 0.74 million, and the VOI of XRF data is \$ 0.84 million. This might make the acquisition of XMET and XRF data useful, depending on the actual prices of acquisition.

We next compute the VOIs as a function of the mining recovery rate and the operation costs in the pit. In Figure 5 we study the VOI of XRF (left) and the difference in VOIs (right), with operation costs (first axis) and the mining recovery (second axis). The results are presented for the three levels of the oxide product price (top, middle and bottom). In this case with a one-stage decision about whether to open the mine or not, the VOIs are high only for a narrow band of mining costs and recovery rates. Parameter settings in this band correspond to prior values near 0, and there is much added value in acquiring more XRF or XMET data. Outside the band the costs are either i) too high, meaning that the oxide resource becomes too expensive to produce, with or without data, or ii) too small, so we would be better off just opening the mine, without collecting more data. At the highest levels, the VOI of XRF is \$ 1.6 million, and the VOI of XMET is just a little bit smaller. The VOI of XRF data is significantly positive for a relatively broader range of cost and recovery parameters (Figure 5, right).

The VOI must be compared with the actual data prices. The drilling cost of the new boreholes is estimated to \$ 0.84 million in this case. The additional price of XRF lab measurements is \$ 0.13 million, and the total price of XRF data is then \$ 0.97 million. Depending on the expected price of the oxide product and the assumed costs and recoveries, we can decide if the additional boreholes are worth the effort. With the specified levels (mining cost \$ 3 million per tonn, mining recovery 95 %), it seems the boreholes might just be valuable if the price of the oxide products is near the

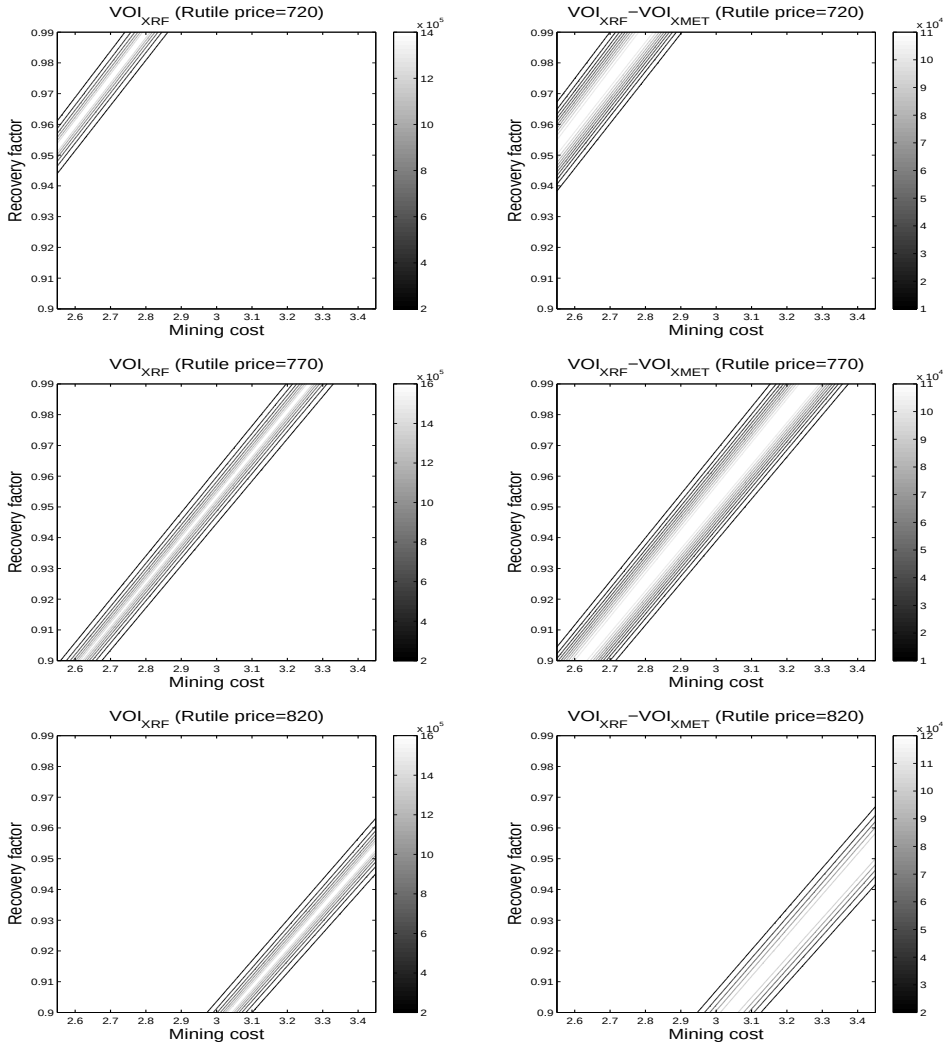

Figure 5: Value of information as a function of the mining costs (first axis) and mining recovery rate (second axis). The value of XRF information (left) and the added value of XRF information compared with XMET information (right). Top: the oxide product price is relatively low. Middle: the oxide product price is intermediate. Bottom: the oxide product price is relatively high.

intermediate range. Only for that oxide price level is the planned XRF or XMET data likely to help us make better decisions about the oxide resource.

In Figure 6 (left) we show the decision regions as a function of XMET and XRF data acquisition prices. This is computed for the intermediate price range of oxide ($ 770 per ton) and for the 95 % recovery rate and 3 million per ton mining cost. The decision regions are computed by selecting the data type that gives the largest added value, compared with the price of data. This entails a selection rule of:

$$\text{Decision} = \text{argmax}\left\{\text{VOI}_{\text{XRF}} - \text{Price}_{\text{XRF}}, \text{VOI}_{\text{XMET}} - \text{Price}_{\text{XMET}}, 0\right\}, \qquad (15)$$

where we decide to purchase XRF if $\text{VOI}_{\text{XRF}} - \text{Price}_{\text{XRF}}$ is the highest element in the length three vector in (15). If none of the first two entries are positive, we decide to purchase no more

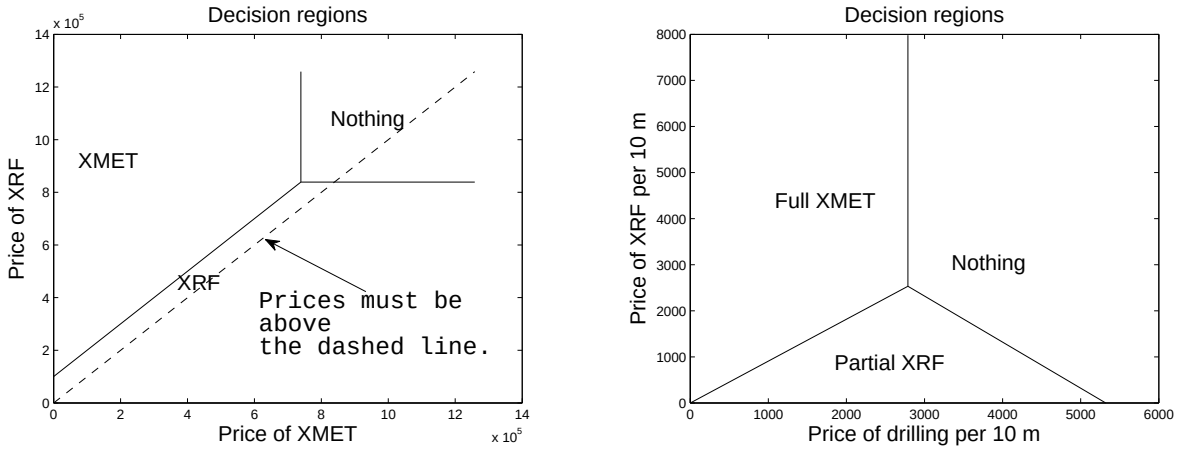

Figure 6: Decision regions. Left: Whether to purchase full XMET or XRF data, or nothing. The first axis represents the price of XMET data. The second axis is the price of XRF data. Right: Whether to purchase XRF in the seven top-ranked boreholes or XMET in all boreholes, or nothing. The first axis represents the price of drilling 10 m. The second axis is the price of processing XRF data per 10 m.

data. In our situation, with $\text{Price}_{\text{XMET}} = \$\,0.84$ million we are just within the 'Nothing' region, and would decide not to purchase this data. Recall that the price of XRF is always higher than the price of XMET, and the relevant price ranges are above the straight line in Figure 6 (left). XRF data is the most lucrative data type for very small laboratory prices. For more expensive laboratory analysis, XMET data is preferable.

5.4 The influence of individual boreholes

We now study the effect of individual boreholes among the planned data. We compute the different evaluation criteria when one borehole is removed from the set of planned holes. This provides a ranking of the individual boreholes in terms of information content.

Table 3 displays the ranking of individual boreholes for all criteria. For the Kriging std criterion

Table 3: The rank of the seven most valuable boreholes based on different criteria: Kriging std, slope, correlation, weight of mean, entropy and the VOI.

	Rank 1	Rank 2	Rank 3	Rank 4	Rank 5	Rank 6	Rank 7
Std	7	8	12	5	16	13	14
Slope	21	1	15	9	16	14	11
Corr	7	21	8	1	16	5	12
Weight	7	8	21	1	16	5	12
Entropy	7	8	19	13	5	12	14
VOI	7	8	5	1	16	11	12

the Rank 1 borehole is the one that causes the largest increase in average prediction uncertainty when it is removed from the set of planned boreholes. For slope the Rank 1 borehole is the one

that causes the largest decrease in average parameter value. Equivalently for correlation, weight of mean and entropy. The Rank 1 borehole for VOI is the one that causes the smallest VOI when it is removed from the set of planned boreholes. Of course, the lengths of the boreholes are important, but note that the measurements within a borehole tend to be very dependent, so it is probably not that interesting to evaluate the value per measurement. The location of boreholes, relative to the current data and the resource blocks is of course relevant.

Borehole 7 and 8 come out as the most informative using most evaluation criteria. Borehole 7 is the longest borehole with 33 observations, borehole 8 has 21 and is the third longest. There are slight variations in the rankings, but the one criteria standing out is the slope which ranks borehole 21 on top, and has 7 and 8 just outside the top seven list. Borehole 21 contains only 11 observations, and is just outside rank 7 in most of the other criteria. A possible explanation for the rankings of slope is the skewed distribution of slope in Figure 4. Removing data will push the slopes away from 1, but the relative effect is not as clear as for the other criteria, especially when considering the average slope. We note that the correlation and weight of the mean criteria appear a bit like the slope, while the more commonly used uncertainty reduction criteria; kriging standard deviation and entropy (and VOI) are different from slope, and quite similar to each other.

We next study the VOI of XRF data in the seven top-ranked boreholes. This is compared with the VOI of XMET data in all 21 boreholes. Like in Section 5.3, we create decision regions for various prices of XRF data and XMET data. For any set of acquisition prices, the decision is to purchase the data with the largest VOI compared with the associated price of data. We compute this as a function of the price of drilling 10m and the (additional) price of XRF processing per 10 m. Figure 6 (right) shows the decision regions of the partial XRF acquisition, full XMET data, or nothing. When the price of XRF processing is small or moderate, compared with the drilling price, we decide to purchase partial XRF data. When the processing price increases, full XMET becomes the most lucrative. If both prices are very large, we decide to purchase no more data.

6 Closing remarks

We have presented a unified geostatistical model for XMET and XRF data used in mining exploration. Several criteria for uncertainty reduction are discussed, and we demonstrate how to compute the value of information in this context by assuming some cost and revenue input. Our case study is from an oxide mineralization in Norway.

We performed an analysis to understand the value of drilling more boreholes, and which data (XRF or XMET) to acquire in these boreholes. Our analysis shows that about 40 million tonnes can be classified as measured or indicated given the planned data. This is a significant increase from the current level. The ore also contains some other minerals that can help justify opening the mine, but the existing and the planned boreholes are not informative of these mineral grades.

The slope parameter seems to be less robust than the others (Kriging standard error, correlation, and weight of the mean), probably because it is very close to 1 for many resource blocks.

The value of information is used to compare XMET and XRF acquisition over assumed costs, recovery factors and price ranges. For the case study the imperfect XMET data is almost as valuable as perfect XRF information, and the XMET comes with a smaller cost. However, neither XRF nor XMET data seem to provide a lot of added value relative to their price ranges and the decision at stake. On the other hand, the VOI is quite sensitive to input parameters in this situation, and for intermediate price ranges, the planned boreholes can be valuable.

The value of information is computed based on the prior and pre-posterior values for a one-time decision: open the entire mine or not. In practice a more complex mining strategy would be incorporated. For instance, it is important to generate cash flow as early as possible. However, one should not only take high-quality ore for a long period of time, because that could lead to a long periode of mining only waste rock. Moreover, one can decide to go underground or to stop based on very uncertain drill cutting grade data collected during mining. In this situation the value of information typically becomes larger, because one is closer to make decisions with huge implications. However, the computation is a complicated expression, where actions depend on the outcomes in a sequential strategy (Miller (1975); Bhattacharjya et al. (2010)). One solution is to use some kind of approximate dynamic programming, while attempting to incorporate the important parts of the mining strategy (Boland et al., 2010).

In this work we have assumed that the joint Gaussian geostatistical model for XRF and XMET is valid. In would be interesting to confirm the imposed correlation in XRF and XMET by analyzing some of the new data both with data types.

7 Acknowledgments

We acknowledge the mining company for letting us use their data.

8 References

Alford C, Brazil M, Lee DH (2007) Optimisation in underground mining. Handbook in Operations Reserach in Natural Resources, Eds. Weintraub et al. .Springer.

Banerjee S, Carlin BK, and Gelfand AE (2004) Hierarchical modeling and analysis for spatial data. Chapman & Hall.

Bhattacharjya D, Eidsvik J, Mukerji T (2010) The value of information in spatial decision making. Mathematical Geosciences 42: 141-163.

Bickel JE (2008) The relationship between perfect and imperfect information in two-action two state systems. Decision Analysis 5: 116-128.

Boland N, Dumitrescu I, Froyland, G (2010) A Multistage Stochastic Programming Approach to Open Pit Mining Production Scheduling with Uncertain Geology. Report. University of Newcastle, Australia.

Bouma JA, van der Woerd HJ, Kuik, OJ (2009) Assessing the value of information for water quality management in the North Sea. Journal of environmental management 90: 1280-1288

Cover TM, Thomas JA (1991) Elements of Information Theory. Wiley.

Cressie N (1993) Statistics for spatial data. Wiley.

Eidsvik J, Bhattacharjya D, Mukerji T (2008) The value of information of seismic amplitude and electromagnetic resitivity data. Geophysics 73: R59-R69.

Froyland G, Menabde M, Stone P, Hodson D (2004) The value of additional drilling to open pit mining projects. Proceedings of Orebody Modelling and Strategic Mine Planning - Uncertainty and Risk Management, Perth, Australia, pp 169-176.

JORC (2004) Australasian Code for Reporting of Exploration Results, Mineral Resources and Ore Reserves. 2004 Edn.

Le ND, Zidek JV (2006) Statistical Analysis of Environmental Space-time processes. Springer.

Mardia KV, Marshall RJ (1984) Maximum likelihood estimation of models for residual covariance functions in spatial regression. Biometrika 73: 135-146.

Martinelli G, Eidsvik J, Hauge R, Førland MD (2011) Bayesian networks for prospect analysis in the North Sea. AAPG Bulletin 95: 1423-1442.

Martinez LA (2009) Why accounting for uncertainty and risk can improve final decision-making in strategic open pit mine evaluation. Project Evaluation Conference. Melbourne, Vic, 21-22 April 2009

Miller AC (1975) The value of sequential information. Management Sciences 22: 1-11.

Phillips J, Newman AM, Walls MR (2009) Utilizing a value of information framework to improve ore collection and classification procedures. The Engineering Economist 54: 50-74.

Pilger GG, Costa JFCL, Koppe JC (2001) Additional samples: where they should be located. Natural resources research 10: 197-207.

Raiffa H (1968) Decision analysis. Addison-Wesley.

Rivoirard J (1987) Two key parameters when choosing the Kriging neighborhood. Mathematical Geology 8: 851-856.

Trainor-Guitton WJ, Caers, JK, Mukerji T (2011) A Methodology for Establishing a Data Reliability Measure for Value of Spatial Information Problems. Mathematical Geosciences 8: 929-949.

Vann J, Jackson S, Bertoli O (2003) Quantitative Kriging neighborhood analysis for the mining geologist - a description of the method with worked case examples. Proceedings of the Fifth International Mining Conference, Bendigo, Vic.

Wellmann JF, Horowitz FG, Regenauer-Lieb K (2011) Towards a Quantification of Uncertainty in 3-D Geological Models. IAMG 2011 Proceedings, doi:10.5242/iamg.2011.0147

Willan AR, Pinto EM (2005) The value of information and optimal clinical trial design. Statistics in Medicine, 24: 1791-1806.

Zimmerman, DL (2006) Optimal network design for spatial prediction, covariance parameter estimation, and empirical predicition. Environmetrics, 17: 635-652.